Takagi-Sugeno fuzzy observer based magnetorheological damper fault diagnosis using a support vector machine

Kicheol Jeong, Seibum B. Choi, *Member, IEEE*

***Abstract*—In this paper, a magnetorheological damper fault diagnosis algorithm is proposed. Recently, various studies have been proposed fault diagnosis methods for this damper system, however, these methods use a displacement sensor in addition to the two accelerometers mounted on the commercial vehicle. The use of this sensor configuration limits the application of the algorithm proposed so far to commercial vehicles. In order to overcome this limitation, the paper proposes a magnetorheological damper fault diagnosis algorithm that uses only two accelerometers. Based on these sensors, the states of the vehicle suspension system are estimated by a Takagi-Sugeno fuzzy unknown input observer. This observer scheme can estimate the states of the damper even under conditions affected by damper hysteresis and unknown road elevation. Using the Lyapunov stability theorem, the stability of the proposed observer with an unmeasured premise variable is verified. In addition, a support vector machine classifier is used to determine damper condition without empirically set thresholds. In this paper, a fault flag is generated by data-driven machine learning algorithms, reducing the design effort while at the same time achieving optimal performance. The proposed algorithm is verified using a quarter-car test rig and test results confirm that the proposed algorithm exhibits robust performance in various road conditions. Consequently, the magnetorheological damper fault diagnosis algorithm proposed in this paper can reduce the effort in designing a diagnosis algorithm while using inexpensive production sensors applied to a vehicle.**

***Index Terms*—fault diagnosis, support vector machine, takagi-sugeno fuzzy observer, vehicle suspension, magnetorheological damper**

NOMENCLATURE

F_{MR}	MR damping force.
a_2	Damping coefficient parameter.
b_1	Weight of scale factor.
b_2	Weight of viscous damping coefficient.
c_1	Bias of scale factor.
c_2	Bias of viscous damping coefficient.
i	MR damper current.
i_a	Actual MR damper current.
i_f	MR damper current fault.
v_{rel}	MR damper velocity.
m_s	Sprung mass.
m_u	Unsprung mass.
z_s	Sprung mass location.
z_u	Unsprung mass location.
z_r	Road elevation.
k_s	Suspension spring coefficient.
k_t	Tire vertical stiffness.
η	MR damper control bandwidth.
F_d	Desired damping force.
F_a	Actual damping force.
ζ	Fault flag value.

Kicheol Jeong is with Korea Automotive Technology Institute, Cheonan-si 31214, South Korea (e-mail: kcjeong@katech.re.kr).

Seibum. B. Choi is with the Korea Advanced Institute of Science and Technology, Daejeon 34141, South Korea (e-mail: sbchoi@kaist.ac.kr).

I. INTRODUCTION

THE suspension is an essential component of a vehicle that improves ride comfort and handling performance. Vehicle suspension systems are classified into passive, active, and semi-active suspensions. First, the passive suspension has a simple structure and low cost. However, the fixed damping characteristics make it difficult to simultaneously satisfy the desired vehicle ride comfort and handling performance. Active suspension [1], on the other hand, affords good performance but has the disadvantages of high cost and large energy consumption. Finally, semi-active suspension [2], which can only change the damping characteristics of the damper, can improve ride comfort and handling performance without energy consumption and additional hardware. Therefore, most vehicle manufacturers use semi-active suspension.

Most semi-active vehicle suspension system uses a continuously variable damper with a solenoid valve to change the damping characteristics of the dampers [3]. On the other hand, a magnetorheological (MR) damper [4]–[7] that uses MR fluid is attracting attention since this type of damper has various advantages such as fast response, wide dynamic range and simple structure [8]. The MR damper uses magnetic particles and fluid to change the damping characteristics by supplying current to the damper. By applying a current to this damper, a magnetic field is generated that causes the change of MR fluid state. This principle of operation allows the MR damper to have the various advantages mentioned above. However, various factors cause MR damper faults, and these faults degrade the control performance of the vehicle suspension system. For example, when magnetic particle sediment is deposited in the damper cylinder, the MR damper does not respond to the current input. In addition, other reasons such as magnetic coil failure and oil leakage also render the control system obsolete.

Contrary to the intention of the control engineer, these faults can make the driving experience unpleasant and reduce driving stability. Therefore, in order to improve the ride comfort and handling performance of a vehicle using MR damper control, an MR damper fault diagnosis algorithm is essential.

Recently, various MR damper fault diagnosis algorithms have been proposed. In particular, model-based fault diagnosis frameworks [9] have been used in most previous studies to overcome the effect of unknown disturbances caused by road elevation. De [10] uses the transmissibility of the vehicle suspension system to diagnose the condition of the MR damper. In this paper, system transmissibility is estimated using a quarter car model and derivative of the displacement sensor. Dong [11] uses a full car model and an adaptive sliding mode control framework to diagnose MR damper faults, but the states of the vehicle suspension used in this paper are generally unmeasurable. In addition, this study ignores the nonlinear characteristics of the MR damper. Varrier [12] uses a parity space approach to diagnose MR damper faults, but this method is vulnerable to system uncertainty. In addition, Hernandez [13] and Tudon [14] propose a method of defining and estimating the fault parameter based on the force generated by the MR damper. As in previous studies, a displacement sensor is used in the above method.

The aforementioned previous studies used a vehicle suspension model such as a quarter car model or full car model and a sensor configuration including a displacement sensor to diagnose the MR damper. The methods presented in previous studies have common limitations. First, most of the algorithms used a sensor configuration with a displacement sensor. Displacement sensor allow the design of robust and simple algorithm for estimating the state of vehicle suspension system. However, in general, a displacement sensor is not used except for a small number of vehicles with air suspension [15] due to packaging and cost issues. In addition, in previous studies, a diagnostic algorithm was constructed under the assumption that the nonlinear characteristics of the MR damper can be ignored or the relative velocity, which is an unknown variable, is known. In conclusion, the previously studied MR damper fault diagnosis algorithms are not applicable to commercial vehicles.

To overcome these limitations, this paper propose a robust Takagi-Sugeno (T-S) fuzzy observer based MR damper fault diagnosis algorithm. the T-S fuzzy modeling technique represents the system dynamics using weighted summation of sub-linear system. In this manuscript, the unknown input observer is designed using linear system control theory. The observer used in this paper is designed based on a quarter car MR suspension model that considers the nonlinear characteristics of the MR damper. Since the quarter car MR suspension model is described as sum of linear system, the linear control technique can be adopted. Unlike previous studies, this observer uses only body and wheel acceleration information. Additionally, this paper also uses the support vector machine (SVM), a widely used machine learning algorithm for classification. In this paper, the features required for the SVM classifier are generated based on the estimated state and MR damper model.

This paper is organized as follows. In section II, the MR suspension system of the vehicle is represented by a T-S fuzzy model. In this section, a tangent hyperbolic MR damper model is used to represent the MR damping force. In section III, a robust T-S fuzzy observer is designed based on the MR suspension model derived in section II. Although the T-S MR suspension model has unmeasured premise variables, the proposed observer is stable and robust against unknown road elevation. In addition, an SVM based decision making process is presented in section. Section IV presents an experimental verification, using a quarter car MR suspension test rig. In conclusion, this paper shows that the proposed diagnosis algorithm provides robust performance under various scenarios.

II. T-S FUZZY MR SUSPENSION MODEL

In this section, the T-S fuzzy MR damper model is derived from the experimental data. First, the experimental equipment and experimental results are introduced. Next, a hyperbolic tangent MR damper model is introduced. The parameters of this model are estimated based on experimental data. Lastly, a T-S fuzzy MR suspension model used for observer design is derived.

A. MR damper test environment

The MR damper experimental data used in this study are obtained from the following experimental environment. In this study, the MR damper produced by vehicle suspension maker NEOTECH is used. This MR damper is tested using a shock dyno from damper test equipment manufacturer CTW Automation. Using this shock dyno, various sine wave tests with amplitude of $\pm$25mm are conducted. Fig. 1 shows the experimental equipment.

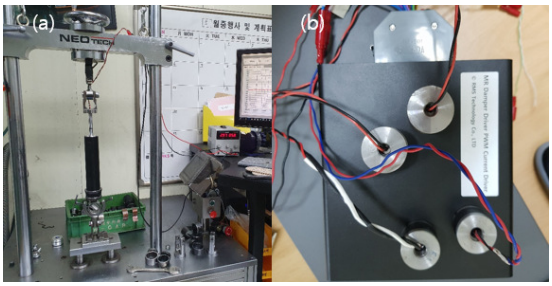

Fig. 1. MR damper test experimental equipment: (a) Shock dyno by CTW Automation (b) MR damper current driver by RMS Technology.

B. Hyperbolic tangent MR damper model

Since the development of the MR damper, various models have been developed to describe the damping characteristics of the MR damper. First, the phenomenological model [16] and the Bouc-Wen model [17] can accurately describe the hysteresis of the MR damper. However, many parameters should be estimated, and the accuracy of the model is highly dependent on the accuracy of the parameter estimation. A polynomial model [18] can simply describe the properties of the MR damper, but an accurate higher order polynomial model has many parameters that must be estimated. On the

other hand, the hyperbolic tangent MR damper model [19] can relatively accurately describe the force of the MR damper with fewer parameters. Therefore, this paper describes the MR damper force using a hyperbolic tangent MR damper model. According to the hyperbolic tangent MR damper model, the force of the MR damper can be described as follows:

$$F_{MR} = (b_1 \cdot i + c_1)\tanh(a_2 \cdot v_{rel}) + (b_2 \cdot i + c_2)v_{rel} \quad (1)$$

where F_{MR} is the damping force of the MR damper, i is the implemented current of the MR damper, and v_{rel} is the relative velocity between sprung mass and unsprung mass. Other variables are model parameters of the hyperbolic tangent MR damper model.

Based on this model described above, model parameters are estimated by the curve fitting method. Table I shows the estimated parameters, Fig. 3 shows the curve fitting results for estimating the MR damper parameter, and Fig. 2 shows the results of the comparison between the hyperbolic tangent MR damping force and the experimental data. In Fig. 3, the experimental data are described by black dots and the R squared value is 0.9872.

TABLE I
HYPERBOLIC TANGENT MR DAMPER MODEL PARAMETERS

Parameter	Estimated value
a_2	23.94
b_1	588.8
b_2	193.5
c_1	381.2
c_2	757.2

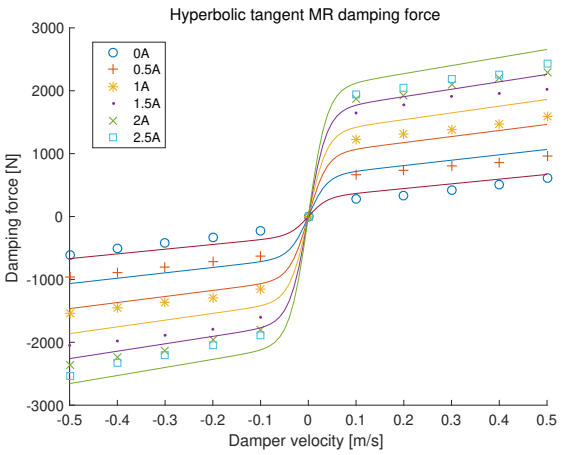

Fig. 2. MR damping force comparison between MR damper test results and hyperbolic tangent MR damper model.

C. T-S fuzzy MR suspension modeling

In this paper, a quarter-car suspension model is used to diagnose the MR damper mounted on the vehicle. The quarter-car model consists of sprung mass and unsprung mass and this model has been used in various vehicle suspension control studies. The governing equations of a quarter-car suspension model such as that in Fig. 4 are as follows:

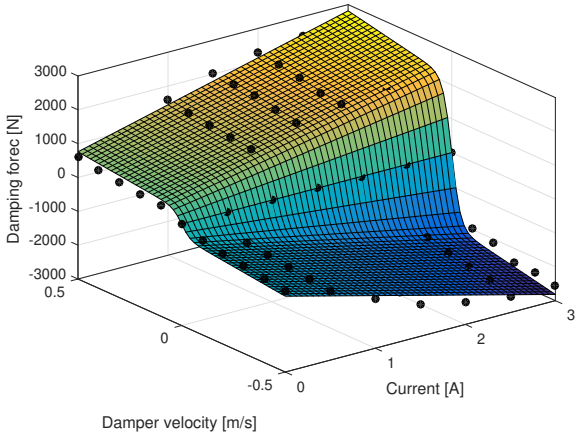

Fig. 3. Curve fitting results for hyperbolic tangent MR damper model parameter estimation.

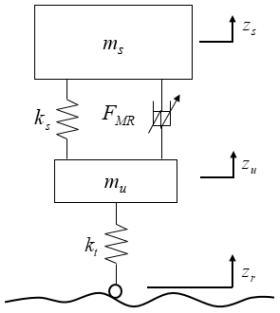

Fig. 4. Quarter-car model of MR suspension system.

$$m_s\ddot{z}_s = -k_s(z_s - z_u) - F_{MR} \quad (2)$$

$$m_u\ddot{z}_u = -k_s(z_u - z_s) + F_{MR} - k_t(z_u - z_r) \quad (3)$$

$$\dot{i} = -\eta(i - u) \quad (4)$$

where m_s is a sprung mass, m_u is an unsprung mass, k_s is the spring stiffness, k_t is the tire vertical stiffness, u is a control command, z_s and z_u are the position of sprung mass and unsprung mass, and z_r is the road elevation. The MR damping force F_{MR} is described by (1). In this paper, the damping effect of the tire is neglected. The physical properties of this model is listed in Table II. According to (4), the actual MR current input is the output of a first order low pass filter. This equation realizes the bandwidth η of the current driver and the MR damper. Using (1) and (2)-(4), the quarter-car MR suspension model is represented in nonlinear state-space form below.

TABLE II
QUARTER-CAR MODEL PROPERTIES

Symbol	Quantity	Value
m_s	Sprung mass	374.03 kg
m_u	Unsprung mass	52.25 kg
k_s	Spring stiffness	22080 N/m
k_t	Tire vertical stiffness	248193 N/m

$$\dot{x} = A(f_1, f_2)x + Bu + D\dot{z}_r \quad (5)$$

$$x = \begin{bmatrix} z_s - z_u & \dot{z}_s & z_u - z_r & z_{\dot{u}} & i \end{bmatrix}^T \tag{6}$$

$$A = \begin{bmatrix} 0 & 1 & 0 & -1 & 0 \\ -\frac{k_s}{m_s} & -\frac{c_{MR}}{m_s} & 0 & \frac{c_{MR}}{m_s} & -\frac{f_1}{m_s} \\ 0 & 0 & 0 & 1 & 0 \\ \frac{k_s}{m_u} & \frac{c_{MR}}{m_u} & -\frac{k_t}{m_u} & -\frac{c_{MR}}{m_u} & \frac{f_1}{m_u} \\ 0 & 0 & 0 & 0 & \eta \end{bmatrix} \tag{7}$$

$$B = \begin{bmatrix} 0 & 0 & 0 & 0 & \eta \end{bmatrix}^T \tag{8}$$

$$D = \begin{bmatrix} 0 & 0 & -1 & 0 & 0 \end{bmatrix}^T \tag{9}$$

$$f_1 = (b_1 \cdot a_2 + b_2)(\dot{z}_s - \dot{z}_u) \tag{10}$$

$$f_2 = \frac{\tanh(a_2 \cdot (\dot{z}_s - \dot{z}_u))}{a_2 \cdot (\dot{z}_s - \dot{z}_u)} \tag{11}$$

where $c_{MR} = c_2 + c_1 a_2 f_2$. In this paper, the sprung mass vertical accelerometer and the unsprung mass vertical accelerometer data are regarded as the measurements of the diagnosis system. These sensors are used by most vehicle manufacturers, and therefore this assumption is reasonable. As in the above equation, the sensor measurement is mathematically described as follows.

$$y = C(f_1, f_2)x = \begin{bmatrix} \ddot{z}_s & \ddot{z}_u \end{bmatrix} \tag{12}$$

$$C(f_1, f_2) = \begin{bmatrix} A_{21} & A_{22} & A_{23} & A_{24} & A_{25} \\ A_{41} & A_{42} & A_{43} & A_{44} & A_{45} \end{bmatrix} \tag{13}$$

In accordance with (5), the MR suspension model takes the form of a nonlinear model. This nonlinear characteristics has to be considered to design a stable observer. In the past several decades, various nonlinear state estimation techniques such as the extended Kalman filter [20], sliding mode observer, [21] and T-S fuzzy modeling [22]–[24] have been proposed. In this paper, the T-S fuzzy model is constructed by the sector nonlinearity technique. According to (10) and (11), the nonlinear terms f_1 and f_2 are bounded. Since the relative velocity of the damper is physically bounded, f_1 is bounded. Next, f_2 has the form of $\tanh x/x$, and therefore this function is bounded from zero to one. In conclusion, the sector nonlinearity technique is used to build the T-S fuzzy model reasonably and the relationship between the premise variable and fuzzy rules can be described as follows.

IF $\dot{z}_s - \dot{z}_u$ is M_1 and z is N_1, THEN $\dot{x} = A_1 x + Bu + D\dot{z}_r$
IF $\dot{z}_s - \dot{z}_u$ is M_1 and z is N_2, THEN $\dot{x} = A_2 x + Bu + D\dot{z}_r$
IF $\dot{z}_s - \dot{z}_u$ is M_2 and z is N_1, THEN $\dot{x} = A_3 x + Bu + D\dot{z}_r$
IF $\dot{z}_s - \dot{z}_u$ is M_2 and z is N_2, THEN $\dot{x} = A_4 x + Bu + D\dot{z}_r$

$$M_1 = (b_1 \cdot a_2 + b_2)(\dot{z}_s - \dot{z}_u) - f_{1\min} \Big/ f_{1\max} - f_{1\min} \tag{14}$$

$$M_2 = 1 - M_1 \tag{15}$$

$$N_1 = \frac{\tanh(a_2 \cdot (\dot{z}_s - \dot{z}_u))}{a_2 \cdot (\dot{z}_s - \dot{z}_u)} - f_{2\min} \Big/ f_{2\max} - f_{2\min} \tag{16}$$

$$N_2 = 1 - N_1 \tag{17}$$

where $f_{1\max}$ and $f_{1\min}$ are the upper bound and lower bound of f_1, and $f_{2\max}$ and $f_{2\min}$ is the upper bound and lower bound of f_2.

Consequently, the quarter-car T-S fuzzy model of the MR suspension is obtained using the above equations and this model is represented by weighted summation of sublinear models.

$$\dot{x} = \sum_{i=1}^{4} h_i(z(t))\,(A_i x + Bu + D\dot{z}_r) \tag{18}$$

$$y = \sum_{i=1}^{4} h_i(z(t)) C_i x \tag{19}$$

$$\begin{aligned} &h_1(z(t)) = M_1 N_1,\ h_2(z(t)) = M_1 N_2, \\ &h_3(z(t)) = M_2 N_1,\ h_4(z(t)) = M_2 N_2 \end{aligned} \tag{20}$$

where $z(t) = [f_1\ f_2]$ is the premise variable and $h_i(z(t))$ is a weighting function that satisfies the following conditions:

$$h_i(z(t)) \in [0\ 1],\ \sum\nolimits_i h_i(z(t)) = 1 \tag{21}$$

It is noteworthy that the premise variable for determining the fuzzy rule is an immeasurable variable. In other words, in order to estimate the state of the MR damper, the fuzzy observer uses the estimated premise variable and satisfies the stability simultaneously.

D. *Uncertainties and disturbances*

Since the quarter car model is an approximation of the vehicle suspension system, there are some uncertainties and disturbances. First, the parametric uncertainty exists in sprung mass since the sprung mass depends on the weight of the passenger. In this paper, the weight of the passenger is assumed 80kg, therefore the sprung mass parameter can have a variability of about 20%. Next, the MR damper force obtained by the hyperbolic tangent model includes uncertainties. Parameters such as unsprung mass, spring coefficient and tire vertical stiffness do not change easily, therefore it is reasonable to assume that there is no or very small uncertainty. Considering the effect of uncertainties on aspects of model stability, the model does not diverge while model uncertainties exist since the sprung mass and MR damper force are bounded and the quarter car model is stable at this boundary. Physically, MR dampers are semi-active dampers that only change the characteristics of the damper, therefore the proposed model can be robust under the influence of model uncertainty since there is no external input force. Furthermore, the coefficients of MR damper force model are likelihood values obtained from various test data. It means that the parametric uncertainties of the MR damper force model is minimized and the coefficients are suitable for depicting the real world MR damper force. This fact is confirmed by the high R squared value of 0.9872 in the model and test data.

A disturbance applied to vehicle suspension system is the road surface elevation. This elevation is the source that vibrates the suspension system and generates MR damping force, however, it is an unknown input that cannot be measured without image sensors or ultrasonic sensors. Therefore, when designing an observer using the model designed in this section, it is necessary to check the stability by considering the unknown input.

III. T-S FUZZY OBSERVER BASE MR DAMPER FAULT DIAGNOSIS

In this section, the T-S fuzzy observer based MR damper fault diagnosis algorithm is proposed. First, a robust unknown input T-S fuzzy observer is designed to estimate the MR damper state. Next, based on the estimated state, SVM based classification is conducted in order to generate a fault flag.

A. T-S fuzzy MR suspension state observer

In order to estimate the state of a nonlinear system, various studies have proposed a T-S fuzzy nonlinear observer [25]–[32]. Previous studies have shown that most studies assume that the premise variable is measurable. However, this kind of algorithm cannot guarantee stability if the premise variable cannot be measured. Therefore, in recent years, various studies on state estimation of T-S fuzzy systems with premise variables that cannot be measured have been conducted [33]–[39]. For instance, Guerra [34] proposed a H_∞ linear matrix inequality (LMI) based T-S fuzzy observer. However, in this previous study, it is assumed that the premise variable and state have a linear mapping relationship. Another study [35] proposed T-S fuzzy observer with multiple output matrices; however, the information of the premise variable is used to obtain measurement information. Therefore, in this paper, a robust unknown input T-S fuzzy observer for unmeasurable premise variables is proposed using the Lipschitz bounded condition. In order to design the T-S fuzzy observer, the T-S fuzzy quarter-car model is divided by four sub-linear models. Based on the definition of the T-S fuzzy system, the state x and measurement y can be described as

$$x(t) = \sum_{i=1}^{4} x_i(t),\ y(t) = \sum_{i=1}^{4} y_i(t) \tag{22}$$

where $x_i(t) = h_i(z(t))x(t)$ and $y_i(t) = h_i(z(t))y(t)$. According to (22), the new variables $x_i(t)$ and $y_i(t)$ depend on the unmeasured premise variable $z(t)$. Therefore, in order to design the T-S fuzzy observer, other variables that depend on the estimated premise variable are defined by

$$\tilde{x}_i(t) = h_i(\hat{z}(t))x(t), \tilde{y}_i(t) = h_i(\hat{z}(t))y(t) \tag{23}$$

where $\hat{z}(t)$ is the estimated premise variable and, according to (20), these new variables satisfy the following condition:

$$x(t) = \sum_{i=1}^{4} \tilde{x}_i(t), y(t) = \sum_{i=1}^{4} \tilde{y}_i(t) \tag{24}$$

Then, using (18), (19), (22) and (24), the T-S fuzzy model can be expressed by

$$\begin{aligned} \dot{x}(t) &= \sum_{i=1}^{4} \dot{x}_i(t) \\ &= \sum_{i=1}^{4} A_i x_i(t) + h_i(z(t))Bu + h_i(z(t))D\dot{z}_r \end{aligned} \tag{25}$$

$$\begin{aligned} y(t) &= \sum_{i=1}^{4} y_i(t) \\ &= \sum_{i=1}^{4} C_i h_i(z(t))x(t) = \sum_{i=1}^{4} C_i x_i(t) \end{aligned} \tag{26}$$

$$\begin{aligned} \dot{x}(t) &= \sum_{i=1}^{4} \dot{\tilde{x}}_i(t) \\ &= \sum_{i=1}^{4} A_i \tilde{x}_i(t) + h_i(\hat{z}(t))Bu + h_i(\hat{z}(t))D\dot{z}_r \end{aligned} \tag{27}$$

$$\begin{aligned} y(t) &= \sum_{i=1}^{4} \tilde{y}_i(t) \\ &= \sum_{i}^{4} C_i h_i(\hat{z}(t))x(t) = \sum_{i}^{4} C_i \tilde{x}_i(t) \end{aligned} \tag{28}$$

Consequently, the sub-linear systems are defined as follows.

$$\begin{aligned} \dot{x}_i(t) &= A_i x_i(t) + h(z(t))Bu + h(z(t))D\dot{z}_r \\ y_i(t) &= C_i x_i(t) \end{aligned} \tag{29}$$

$$\begin{aligned} \dot{\tilde{x}}_i(t) &= A_i \tilde{x}_i(t) + h(\hat{z}(t))Bu + h(\hat{z}(t))D\dot{z}_r \\ \tilde{y}_i(t) &= C_i \tilde{x}_i(t) \end{aligned} \tag{30}$$

Using these sub-linear systems, the observer system proposed in this paper is described in the following form.

$$\begin{aligned} \dot{\mu}_i(t) &= N_i \mu_i(t) + h_i(\hat{z}(t)) + L_i \tilde{y}_i(t) \\ \hat{x}_i(t) &= \mu_i(t) - F_i \tilde{y}_i(t) \end{aligned} \tag{31}$$

The estimated state is then represented as

$$\hat{x}(t) = \sum_{i=1}^{4} \hat{x}_i(t) \tag{32}$$

According to (18), (19) and (23) the difference between (22) and (24) is weight part h. In (22), the sub-state $x_i(t)$ and sub-measurement $y_i(t)$ are weighted value using $h_i(z(t))$. Therefore, $x_i(t)$ and $y_i(t)$ depend on unmeasured premise variable $z(t)$. In contrast, $\tilde{x}_i(t)$ and $\tilde{y}_i(t)$ in (24) are weighted value using $h_i(\hat{z}(t))$. It means that the state is sum of sub-state which depends on estimated premise variable $\hat{z}(t)$). It is noteworthy that the error dynamics can be expressed by estimated premise variable by using (24). Consequently, it is possible to design stable observer using error dynamics which is function of the estimated premise variable. In this paper, the sub-linear systems (29) and (30) are observable. In order to design observer matrices, a stability analysis based on error dynamics should be conducted. In accordance with (29)-(31), the error dynamics of the observer system is obtained by

$$e_i(t) = \hat{x}_i(t) - x_i(t) \tag{33}$$

$$e_i(t) = \mu_i(t) - F_i \tilde{y}_i(t) - x_i(t) + (F_i y_i(t) - F_i y_i(t)) \tag{34}$$

$$e_i(t) = \mu_i(t) - M_i x_i(t) - F_i C_i(\tilde{x}_i(t) - x_i(t)) \tag{35}$$

where $M_i = I + F_i C_i$. The error dynamics is expanded using (31) and (35).

$$\begin{aligned} \dot{e}_i &= \dot{\mu}_i - M_i \dot{x}_i - F_i C_i(\dot{\tilde{x}}_i - \dot{x}_i) \\ &= N_i \mu_i + h_i(\hat{z}) G_i u + L_i \tilde{y}_i - M_i\ \dot{x}_i - F_i C_i(\dot{x}_i - \dot{x}_i) \end{aligned} \tag{36}$$

Using (29) and (30), this error dynamics can be expressed by

$$\begin{aligned} \dot{e}_i = N_i e_i &+ (N_i M_i - M_i A_i + L_i C_i) x_i \\ &+ (N_i F_i C_i + L_i C_i - F_i C_i A_i)(\tilde{x}_i\ - x_i) \\ &+ h_i(\hat{z})(G_i - M_i B)u + (h_i(\hat{z}) - h_i(z))Bu \\ &- F_i C_i(\ h_i(\hat{z}) - h_i(z))D\dot{z}_r - h_i(z) M_i D\dot{z}_r \end{aligned} \tag{37}$$

In order to design observer matrices that make the T-S fuzzy observer stable, Theorem 1 and Lemma 1 are used.

Lemma 1: For any real matrices X, Y and a positive definite matrix P, the following equation always holds [40]:

$$X^TY + Y^TX \leq X^TPX + Y^TP^{-1}Y \tag{38}$$

Theorem 1: For a given positive scalar ρ, the T-S fuzzy observer (31) is asymptotically stable if there exist a positive scalar λ and the positive definite matrix P satisfying the following conditions.

$$N_iM_i - M_iA_i + L_iC_i = 0 \tag{39}$$

$$G_i - M_iB = 0 \tag{40}$$

$$M_iD = 0 \tag{41}$$

$$\begin{bmatrix} H_i^{11} & 0 \\ 0 & H_i^{22} \end{bmatrix} < 0 \tag{42}$$

$$\left\| \begin{bmatrix} (h_i(\hat{z}) - h_i(z))\,u & (h_i(\hat{z}) - h_i(z))\,\dot{z}_r \end{bmatrix} \right\| \leq \rho \left\| e_i \right\| \tag{43}$$

where

$$H_i^{11} = \bar{N}_i^TP + P\bar{N}_i + \bar{N}_i^TP\bar{N}_i + \lambda\rho^2 I \tag{44}$$

$$H_i^{22} = \bar{M}_i^TP\bar{M}_i - \lambda I \tag{45}$$

$$\bar{N} = \begin{bmatrix} N & N-A \\ 0 & A \end{bmatrix} \tag{46}$$

$$\bar{M} = \begin{bmatrix} -B & -D \\ B & D \end{bmatrix} \tag{47}$$

Proof)
Under conditions (39)-(41), the error dynamics (37) is rewritten as

$$\begin{aligned} \dot{e}_i = {} & N_ie_i + (N_i - A_i)(x_i - \tilde{x}_i) \\ & -(h_i(z) - h_i(\hat{z}))Bu - (h_i(z) - h_i(\hat{z}))D\dot{z}_r \end{aligned} \tag{48}$$

In order to design a stable T-S fuzzy observer, another error dynamics is defined as

$$\begin{aligned} \dot{\tilde{e}} &= A_i\tilde{x}_i + h_i(\hat{z})Bu + h_i(\hat{z})D\dot{z}_r \\ &\quad -(A_ix_i + h_i(z)Bu + h_i(z)D\dot{z}_r) \\ &= A_i\tilde{e} + (\ h_i(\hat{z}) - h_i(z))Bu + (h_i(\hat{z}) - h_i(z))D\dot{z}_r \end{aligned} \tag{49}$$

where $\tilde{e} = \tilde{x}_i - x_i$. The augment error is then defined as $\bar{e}_i = \begin{bmatrix} e_i & \tilde{e}_i \end{bmatrix}^T$. Consequently, the augmented error dynamics is defined as

$$\begin{aligned} \begin{bmatrix} \dot{e}_i \\ \dot{\tilde{e}}_i \end{bmatrix} &= \begin{bmatrix} N_i & -N_i + A_i \\ 0 & A_i \end{bmatrix} \begin{bmatrix} e_i \\ \tilde{e}_i \end{bmatrix} \\ &\quad + \begin{bmatrix} B_i & D_i \\ B_i & D_i \end{bmatrix} \begin{bmatrix} (h_i(\hat{z}) - h_i(z))u \\ (h_i(\hat{z}) - h_i(z))d_i \end{bmatrix} \end{aligned} \tag{50}$$

Then,

$$\dot{\bar{e}} = \sum_{i=1}^{4} \dot{\bar{e}}_i = \sum_{i=1}^{4} \bar{N}_i\bar{e}_i + \bar{M}_i\Lambda_i \tag{51}$$

where

$$\bar{e}_i = \begin{bmatrix} \dot{e}_i \\ \dot{\tilde{e}}_i \end{bmatrix},\ \Lambda_i = \begin{bmatrix} (h_i(\hat{z}) - h_i(z))u \\ (h_i(\hat{z}) - h_i(z))d_i \end{bmatrix}$$

$$\bar{N}_i = \begin{bmatrix} N_i & -N_i + A_i \\ 0 & A_i \end{bmatrix},\ \bar{M}_i = \begin{bmatrix} B_i & D_i \\ B_i & D_i \end{bmatrix}$$

In this paper, the T-S fuzzy observer is designed using the Lyapunov stability theorem. According to the above equations, the Lyapunov function can be defined as

$$\begin{aligned} \dot{V}(t) &= \sum_{i=1}^{4} \dot{\bar{e}}_i^T(t)P\bar{e}_i(t) + \bar{e}_i^T(t)P\dot{\bar{e}}_i(t) \\ &= \sum_{i=1}^{4} (\bar{N}_i\bar{e}_i + \bar{M}_i\Lambda)^TP\bar{e}_i + \bar{e}_i^TP(\bar{N}_i\bar{e}_i + \bar{M}_i\Lambda) \end{aligned} \tag{52}$$

Using (52) and *Lemma* 1, the following inequality is derived.

$$\begin{aligned} \dot{V} \leq \sum_{i=1}^{4} (\bar{e}_i^T & \left[\bar{N}_i^TP + P\bar{N}_i\right]\bar{e}_i \\ & + \bar{e}_i^T\bar{N}_i^TP\bar{N}_i\bar{e}_i + \Lambda^T\bar{M}_i^TP\bar{e}_i + \bar{e}_i^TP\bar{M}_i\Lambda) \end{aligned} \tag{53}$$

According to (43), the uncertainty from the unmeasured premise variable is Lipschitz bounded in $e_i(t)$. Therefore, the Lyapunov function can be rewritten as

$$\begin{aligned} \dot{V} \leq \sum_{i=1}^{4} \bar{e}_i^T & \left[\bar{N}_i^TP + P\bar{N}_i + \bar{N}_i^TP\bar{N}_i + P + \lambda\rho^2 I\right]\bar{e}_i \\ & + \Lambda^T\left[\bar{M}_i^TP\bar{M}_i - \lambda I\right]\Lambda \end{aligned} \tag{54}$$

$$\dot{V}(t) \leq \sum_{i=1}^{4} \left(\begin{bmatrix} \bar{e}_i^T \\ \Lambda_i^T \end{bmatrix} \begin{bmatrix} H_i^{11} & 0 \\ 0 & H_i^{22} \end{bmatrix} \begin{bmatrix} \bar{e}_i & \Lambda_i \end{bmatrix} \right) \tag{55}$$

Therefore, if the proposed T-S fuzzy observer satisfies the condition (42), this observer is asymptotic stable. In this paper, Matlab LMI toolbox YALMIP/MOSEK is utilized to solve LMI (42). Since this equation has the form of bilinear matrix inequality, this condition is transformed into LMI form using Schur complement [41]. Condition (42) can then be transformed by

$$\begin{bmatrix} H_i^{11} & 0 \\ 0 & H_i^{22} \end{bmatrix} < 0 \Leftrightarrow \begin{bmatrix} S_i^{11} & 0 \\ 0 & S_i^{22} \end{bmatrix} < 0 \tag{56}$$

where

$$S_i^{11} = \begin{bmatrix} \bar{N}_i^TP + P\bar{N}_i + \lambda\rho^2 I + P & \bar{N}_i^TP \\ P\bar{N}_i & -P \end{bmatrix}$$

,

$$S_i^{22} = \begin{bmatrix} -\lambda I & \bar{M}_i^TP \\ P\bar{M}_i & -P \end{bmatrix} \tag{57}$$

B. Learning data extraction based on the T-S fuzzy observer

It is noteworthy that the T-S fuzzy observer designed in the previous subsection is robust against unknown road elevation as well as control input. According to (40), this constraint ensures that the control input does not affect the error dynamics of the observer. Since condition (40) is satisfied, the input term $h_i(\hat{z})(G_i - M_iB)u$ is decoupled from error dynamics (37). This means that the estimated states of the MR damper do not depend on the fault input. In this paper, this property of the observer is utilized to extract the feature used for MR damper diagnosis. Using the observer and hyperbolic tangent model, the damping force of MR damper is obtained as follows.

$$\begin{aligned} \hat{F}_d(i_c, \dot{\hat{z}}_s - \dot{\hat{z}}_u) &= (b_2i_c + c_2)(\dot{\hat{z}}_s - \dot{\hat{z}}_u) \\ &\quad + (b_1i_c + c_1)\tanh(a_2(\dot{\hat{z}}_s - \dot{\hat{z}}_u)) \end{aligned} \tag{58}$$

$$i_c = i_a + i_f \tag{59}$$

where i_c is the current control command, i_a is the actually implemented current of the MR damper, i_f is the faulty current of the MR damper, and F_d is the MR damping force expected to be implemented by the control. In this paper, the MR damper force is represented using the fault current input. According to (58), the desired damping force F_d is a function of the faulty current i_f. On the other hand, the actual damping force F_a can be represented using a quarter-car model such as

$$\hat{F}_a = -k_s(\hat{z}_s - \hat{z}_u) - m_s\ddot{\hat{z}}_s \tag{60}$$

As mentioned above, the faulty current i_f does not have an impact on the estimated states. Therefore, F_a is an accurate estimate of the actual force of the MR damper with or without a fault. In accordance with (58) and (60), the desired damping force F_d is equal to the actual damping force F_a if the MR damper is fault-free. On the other hand, when an MR damper fault occurs, the actual damping force of the MR damper is less than the desired damping force. Consequently, the fault flag ζ that indicates the MR damper fault can be generated as follows.

$$\zeta = \begin{cases} 1, & F_d \neq F_a \\ 0, & F_d = F_a \end{cases} \tag{61}$$

C. SVM based fault determination

Theoretically, the MR damper fault can be detected using (61). In practice, however, unexpected model uncertainties, unknown input and sensor noise degrade the performance of the diagnostic algorithm. Therefore, if the fault diagnosis algorithm is completely dependent on (61), then a false alarm problem arises. Consequently, an algorithm that can determine the fault using information obtained from the observer and model is needed. In many previous studies, a fixed threshold is utilized to overcome the effect of disturbances. However, it takes a lot of effort to determine the threshold for optimal performance. Therefore, this paper proposes a SVM based fault determination method. SVM is a kind of machine learning algorithm optimized for binary classification and requiring a relatively small amount of data [42]. Fig. 5 shows the concept of the SVM classifier. The SVM creates decision boundaries that divide the data based on input features. In the SVM theory, the nearest data is named a support vector. The SVM determines the decision boundary by solving an optimization problem that maximizes the margin between the support vector and the decision boundary.

SVM is divided into different types depending on the kernel function [43] used in the optimization technique. In this paper, the Gaussian radial basis function (RBF) used for SVM learning. In this paper, the hyper parameter of the learning algorithm is determined by considering the characteristics of the data.

D. Data preprocessing

In the field of machine learning, data preprocessing [44] is an essential process to enhance the performance of machine learning. In particular, data preprocessing makes the machine learning model more accurate and reduces the training time. In fact, most research on machine learning applications has

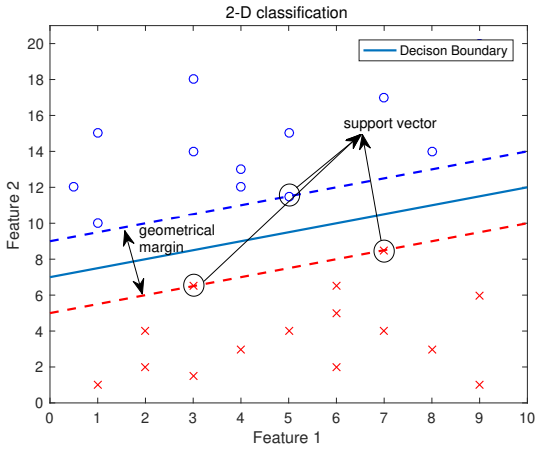

Fig. 5. Two class classification of support vector machine.

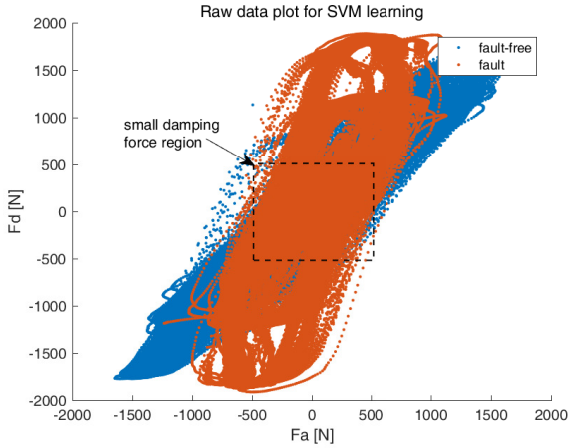

Fig. 6. Scatter plot of raw data: desired force by actual force.

conducted data preprocessing. Fig. 6 shows the scatter plot of the raw data obtained by (58) and (60). In accordance with this figure, there is a region where fault data and fault-free data overlap. This region appears since the impact of a fault on the MR suspension system decreases when the relative velocity of the MR damper is low. In other words, the fault of the MR damper cannot be detected without the movement of the MR damper. This overlapped data makes a machine learning model approach inaccurate and delays training time. In order to overcome this problem, in this paper, data processing using a moving average filter is conducted.

Fig. 7 shows the result of data preprocessing. In this paper, the absolute value of raw data is filtered through a moving average filter. According to Fig. 7, data overlapping is reduced. In addition, in this paper, fault data with absolute values of the desired damping force of less than 250 N are dropped. This process can contribute to improving machine learning performance as follows. First, the learning time of machine learning algorithms can be greatly reduced by dropping fault data in the region where data overlapping occurs most. Furthermore, this data dropping reduces the risk of false alarms caused by the SVM classifier. In fact, the fault diagnosis algorithm

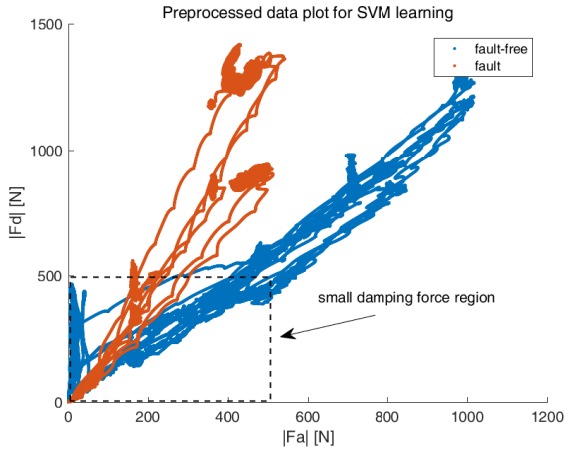

Fig. 7. Scatter plot of preprocessed data: desired force by actual force.

used in vehicle systems should be designed to minimize false alarms where faults are detected in the absence of an actual fault. From an accuracy point of view, this data processing can reduce the accuracy of the algorithm in regions which $|F_d|$ less than 250 N. However, since the purpose of the fault diagnosis algorithm is to provide effective information to the driver, accurate fault decision should be made in the area where the damper affects the vehicle system. Physically, if the force of the damper is small, the fault of the damper cannot be detected. As an extreme case, it does not matter if the damper is fault or healthy, in a situation where no damper force occurs, which means that there is no road elevation. Therefore, it is reasonable not to judge the fault of the damper in the region where the damping force is small. As mentioned above, the proposed data preprocessing method can reduce the risk of false alarms by allowing the SVM to determine that the data are fault-free in areas where the fault of the MR damper cannot be diagnosed. In conclusion, it can be expected that the performance of SVM training using preprocessed data is enhanced. The proposed MR damper fault diagnosis algorithm is implemented as shown in Fig. 8.

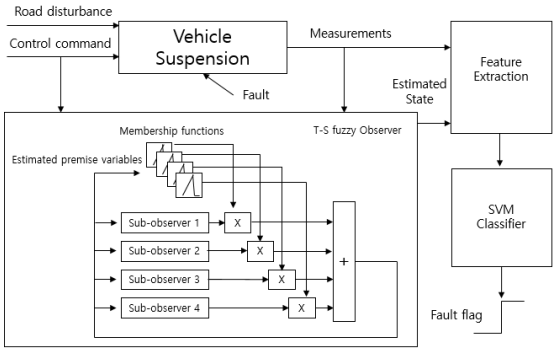

Fig. 8. Schematic description of the MR damper fault diagnosis algorithm.

IV. Experimental Validation

In this section, experimental validation results are introduced using a quarter-car MR suspension test rig. This section is organized as follows. First, the T-S fuzzy observer based feature extraction performance is verified using experimental results. Next, SVM learning is conducted using the sensor signal and features obtained with the proposed observer. For comparison with the fixed threshold method, the data in Fig. 7 is used to determine a fixed threshold. According to Fig. 7, it is confirmed that $|F_a|$ and $|F_d|$ have a linear relationship. Therefore, the fixed threhsold is designed by linear regression. If the MR damper is healthy, the relationship between $|F_a|$ and $|F_d|$ can be described by

$$|F_d| \simeq 1.1468|F_a| \tag{62}$$

Conversely, if the MR damper has a fault, the relationship between $|F_a|$ and $|F_d|$ can be described as

$$|F_d| \simeq 2.6077|F_a| \tag{63}$$

Therefore, the fixed threshold can be designed as

$$|F_d| = 1.8772|F_a| \tag{64}$$

Note that this decision boundary is not fixed in time-force domain. However, this is fixed in actual force-desired force domain. Consequently, using fixed threshold method, the fault flag is generated when $|F_d|$ is larger than $1.8772|F_a|$. In this paper, the experimental road input consists of sine wave, sine sweep and rectangular wave roads. Finally, the performance of the SVM classifier is measured using the $F_{0.5}$ measure, which is a well-known machine learning performance index.

A. Experimental set-up

In order to verify the proposed MR damper diagnosis algorithm, a quarter-car test rig is used, which is widely used to develop suspension control systems in many previous studies. In this study, the customized MR damper for the Hyundai Genesis Coupe is used. In order to obtain actual states such as the suspension displacement and relative velocity, a linear variable differential transformer (LVDT) SLS 130 is attached to the test rig. In addition, MANDO accelerometers, which are actually used in the Hyundai midsize coupe, are attached to a sprung mass and an unsprung mass. The measuring range of the sprung mass accelerometer is ± 2 g and the measuring range of the unsprung mass accelerometer is ± 50 g.
The experimental validation is performed under various road types. First, a sine wave road test was performed to evaluate the performance of the proposed fault diagnosis algorithm in a low frequency range. Next, a 0.5 hz rectangular wave road test with and elevation of -0.01 meter to 0.01 meter was performed. Finally, a sine sweep road test with an elevation of -0.01 meter to 0.01 meter was performed to evaluate the performance of the proposed fault diagnosis algorithm in a

high frequency range. In order to realize the fault of the MR damper, a current input different from the current command input to the estimator was implemented in the MR damper. Fig. 9 shows the experimental equipment for verifying the fault diagnosis performance. The physical characteristics of the quarter-car test rig are listed in Table II.

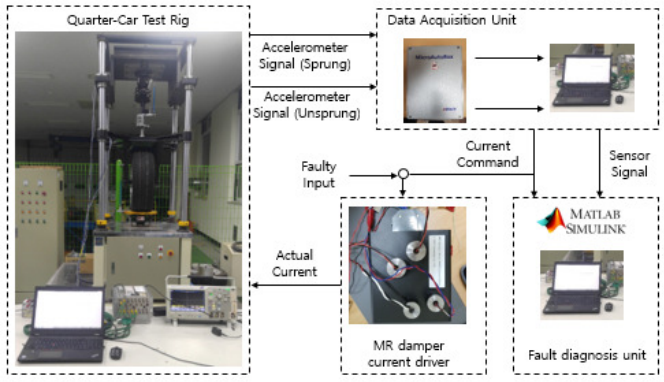

Fig. 9. Overall experimental environment for validating MR damper fault diagnosis algorithm.

B. Experimental results

1) Sine wave test results: Fig. 10 and Fig. 11 show the results of a 3 hz sine wave test with an amplitude of 0.1 meter. First, Fig. 10 shows the fault diagnosis results when an MR damper fault occurs between 15.71 seconds and 35.31 seconds. In this region, the MA damper controller inputs a 1 A current command to the current driver, but the MR damper current does not achieve 1.06 A. According to this figure, it can be confirmed that the proposed T-S fuzzy observer has robust performance in both fault and fault-free regions. As mentioned above, the filtered MR damping force $|F_d|$ and $|F_a|$ have similar value in the fault-free region. On the other hand, the difference between $|F_d$ and $|F_a|$ increases in the fault region. Using this feature, the proposed SVM classifier correctly generates a fault flag. Next, Fig. 11 shows the fault diagnosis results when an MR damper fault occurs after 25.59 seconds. In this figure, due to the model uncertainty of the hyperbolic tangent MR damper model, it can be seen that $|F_d|$ and $|F_a|$ are slightly different, even if no fault occurs. However, in the fault region, the value of $|F_d|$ and $|F_a|$ show a large difference. Therefore, it can be confirmed that the fault diagnosis using the SVM is performed correctly. According to these experimental results, fault determination is slightly delayed due to data preprocessing. However, this slight delay is not critical in the field of suspension fault diagnosis. According to this experimental results, fault diagnosis using SVM can provide improved accuracy compared to traditional fixed-threshold methods. In this experiment, the difference between the existing method and the proposed method is noticeable in the region where the damper force is small. It means that the proposed method can reduce false alarms compared to the fixed threshold method.

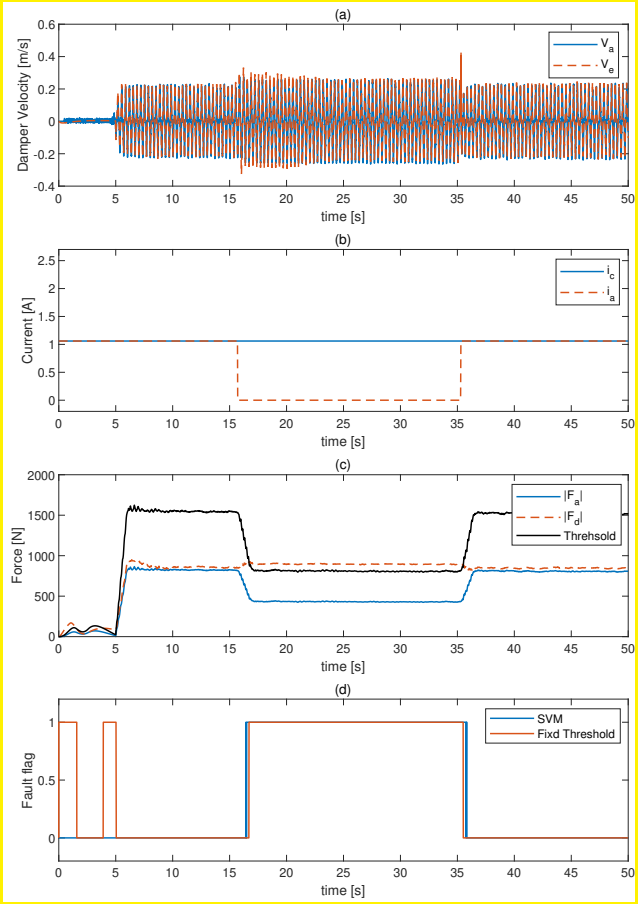

Fig. 10. Sine wave test results for MR damper fault diagnosis: (a) Relative velocity of MR damper (V_a) and estimated relative velocity (V_e) (b) Current command (i_c) and actual MR damper current (i_a) (c) filtered actual MR damping force ($|F_a|$), filtered desired MR damping force ($|F_d|$) and fixed threshold (d) fault flag obtained by SVM and fixed threshold.

2) Rectangular wave test results: Fig. 12 and Fig. 13 show the results of a 0.5 hz rectangular wave test with an amplitude of 0.1 meter. As in the previous experiment, it can be confirmed that the desired damping force and the actual damping force used in the fault diagnosis of the MR damper are robustly estimated. Generally, the rectangular road input increases the variance of the damping force. However, since moving average filtering is used in this paper, the variance of the preprocessed MR damping force is not large. This feature makes the SVM create an accurate model based on the data. Although SVM and fixed threshold method utilize the same signal, it is confirmed that the SVM based fault diagnosis method has better performance comparing with the fixed threshold method. In particular, in the region where the fault occurs, the SVM robustly generates a fault flag despite the vibration of the road surface. Consequently, it is confirmed that the fault flag that indicates an MR damper fault is accurately generated using the SVM classifier.

3) Sine sweep test results: Fig. 14 and Fig. 15 show the results of a 0 hz to 5 hz sine sweep test with an amplitude of 0.1 meter. According to these figures, the proposed T-S fuzzy

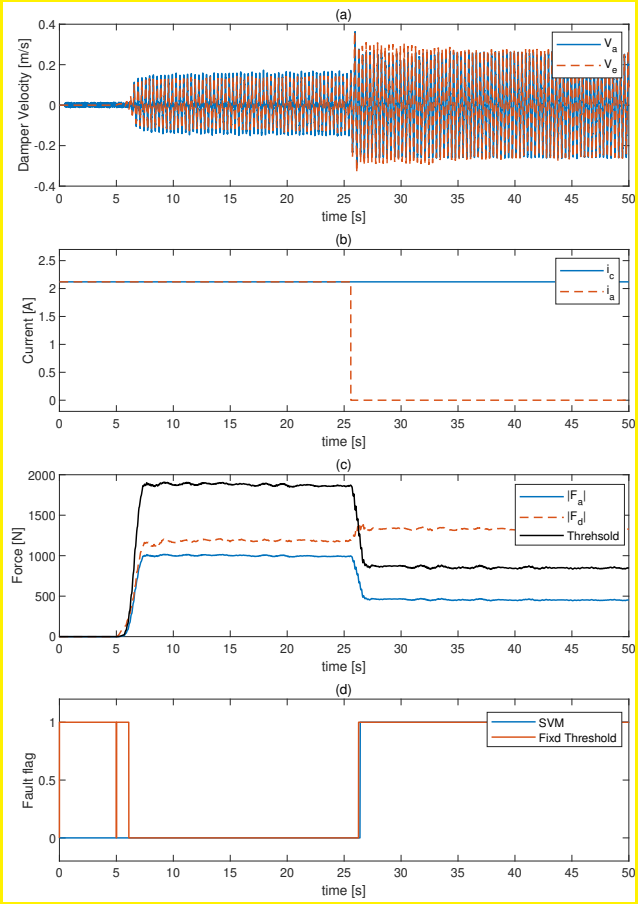

Fig. 11. Sine wave test results for MR damper fault diagnosis: (a) Relative velocity of MR damper (V_a) and estimated relative velocity (V_e) (b) Current command (i_c) and actual MR damper current (i_a) (c) filtered actual MR damping force ($|F_a|$), filtered desired MR damping force ($|F_d|$) and fixed threshold (d) fault flag obtained by SVM and fixed threshold.

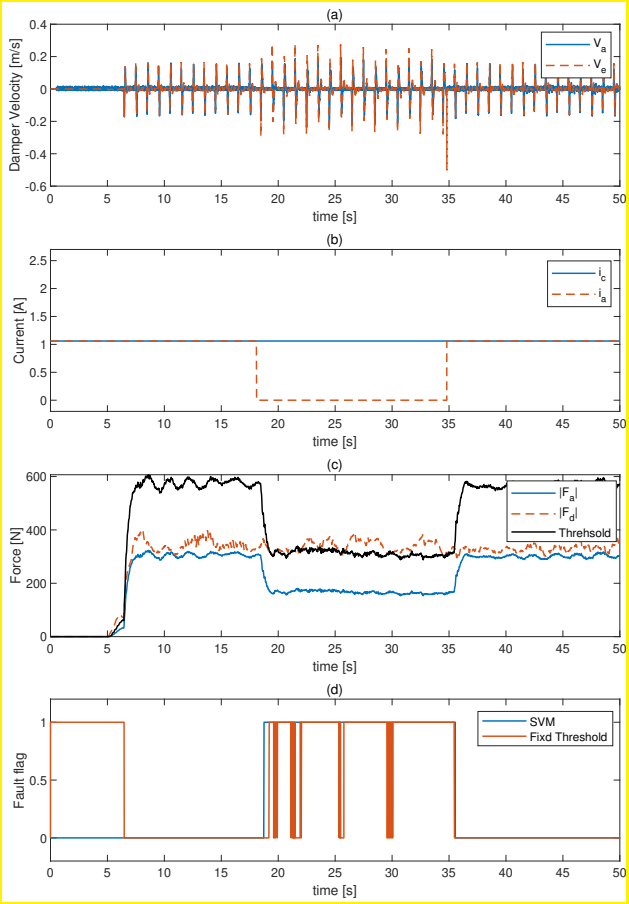

Fig. 12. Rectangular wave test results for MR damper fault diagnosis: (a) Relative velocity of MR damper (V_a) and estimated relative velocity (V_e) (b) Current command (i_c) and actual MR damper current (i_a) (c) filtered actual MR damping force ($|F_a|$), filtered desired MR damping force ($|F_d|$) and fixed threshold (d) fault flag obtained by SVM and fixed threshold.

observer has robust performance in various frequency ranges. Since moving average filtering is employed, the preprocessed damping force data tends to increase as the velocity of the MR damper increases. As with the previous experimental results, the fault flag is correctly generated. The experimental results show that there is significant performance difference between the SVM-based method and the fixed-threshold method in the region where the MR damper current drop is large. When the current in the MR damper drops significantly, $|F_a|$ becomes smaller than $|F_d|$. As a result, in this situation, $|F_d|$ can be less than $1.8772|F_a|$ despite the fault occurring situation.

4) SVM learning results: In this paper, the authors propose an MR damper fault diagnosis method using a SVM classifier. In the above experiments, the kernel function used for SVM learning is Gaussian RBF with a kernel scale of 2. The data used for SVM training consists of a total of 543798 data sets for various fault scenarios. In the field of machine learning, time window is used to extract features from time series signals. Using this time window, features such as mean, variance and frequency response is extracted. In this respect, the sample used in this paper contains the average of the absolute values of the desired damping force and the actual damping force, current command and the value of accelerometer signals. The filtered force values are extracted through a moving average filter with a time window of 1 second. Other signals can be obtained by control unit. In this paper, the five-fold cross validation and the $F_{0.5}$ measure are used to verify the performance of the designed classifier. The $F_{0.5}$ measure is a performance measure that emphasizes precision over recall. Using this performance measure in this paper is reasonable since the fault diagnosis in vehicle system aims at reducing the presence of false alarms as well as accurate fault diagnosis. Using this performance measure, the trained SVM classifier has a $F_{0.5}$ measure of 0.99. Consequently, using this performance measure, it is verified that the proposed SVM classifier has robust performance in MR damper fault diagnosis.

Table III shows the overall experimental result and Fig. 16 shows the result of SVM training as a confusion matrix. Table III shows accuracy and $F_{0.5}$ measure of SVM based and fixed threshold based fault determination. According to this table, it is confirmed that the propose fault determination method using SVM has better performance comparing with the fixed

TABLE III
OVERALL EXPERIMENTAL RESULTS UNDER VARIOUS ROAD CONDITIONS

Road type	Accuracy(SVM)	Accuracy(Fixed)	$F_{0.5}$measure(SVM)	$F_{0.5}$measure(Fixed)	RMS error
Sine wave-1	0.9744	0.9215	0.9676	0.8381	0.0332
Sine wave-2	0.9834	0.8645	1.0000	0.7549	0.0276
Rectangular-1	0.9720	0.8081	0.9458	0.6380	0.0308
Rectangular-2	0.9901	0.8567	1.0000	0.7468	0.0301
Sine sweep-1	0.9703	0.8632	0.9590	0.7714	0.0517
Sine sweep-2	0.9798	0.8716	1.0000	0.7430	0.0513

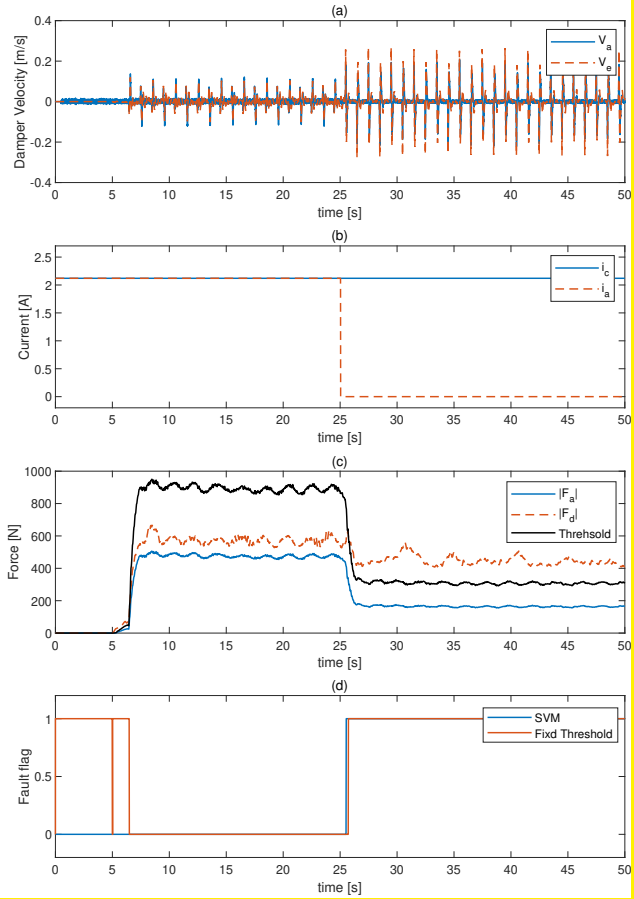

Fig. 13. Rectangular wave test results for MR damper fault diagnosis: (a) Relative velocity of MR damper (V_a) and estimated relative velocity (V_e) (b) Current command (i_c) and actual MR damper current (i_a) (c) filtered actual MR damping force ($|F_a|$), filtered desired MR damping force ($|F_d|$) and fixed threshold (d) fault flag obtained by SVM and fixed threshold.

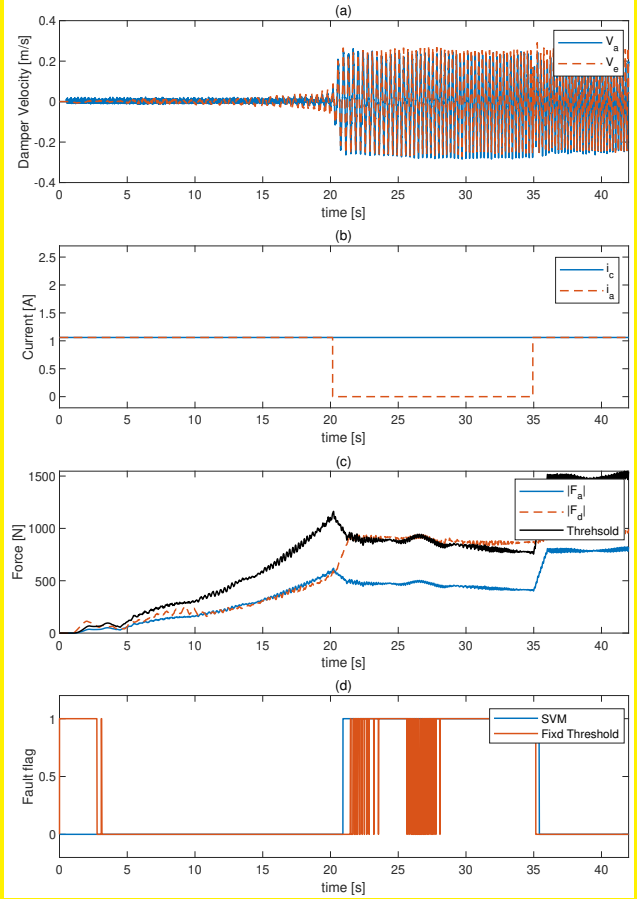

Fig. 14. Sine sweep test results for MR damper fault diagnosis: (a) Relative velocity of MR damper (V_a) and estimated relative velocity (V_e) (b) Current command (i_c) and actual MR damper current (i_a) (c) filtered actual MR damping force ($|F_a|$), filtered desired MR damping force ($|F_d|$) and fixed threshold (d) fault flag obtained by SVM and fixed threshold.

threshold method. In this paper, the T-S fuzzy unknown input observer based MR damper state estimation algorithm is proposed. Furthermore, it is confirmed that the proposed MR damper state estimation algorithm has small root mean square error under various road condition and fault situation. In accordance with Fig. 16, it can be seen that the false-positive error and true-negative error occur with similar frequency. Due to the characteristics of the fault diagnosis algorithm based on the damping force proposed in this paper, it is difficult to diagnose the system condition in the region where the damping force of the MR damper is small. As mentioned above, when the damping force of the MR damper is small, the effect of the fault on the vehicle suspension system is reduced. As a result of SVM training, most of errors occurred within the small damping force region shown in Fig. 6 and Fig. 7.

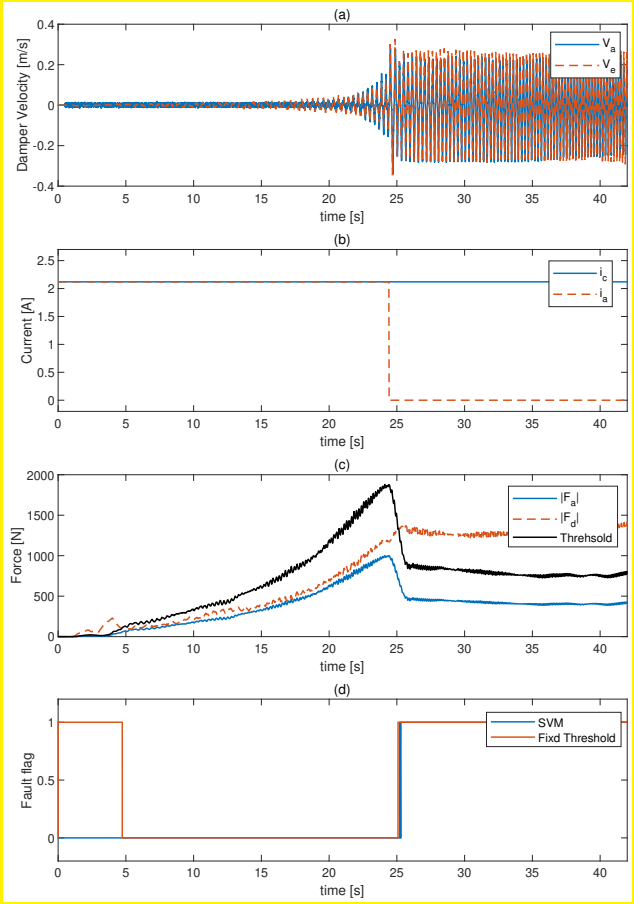

Fig. 15. Sine sweep test results for MR damper fault diagnosis: (a) Relative velocity of MR damper (V_a) and estimated relative velocity (V_e) (b) Current command (i_c) and actual MR damper current (i_a) (c) filtered actual MR damping force ($|F_a|$), filtered desired MR damping force ($|F_d|$) and fixed threshold (d) fault flag obtained by SVM and fixed threshold.

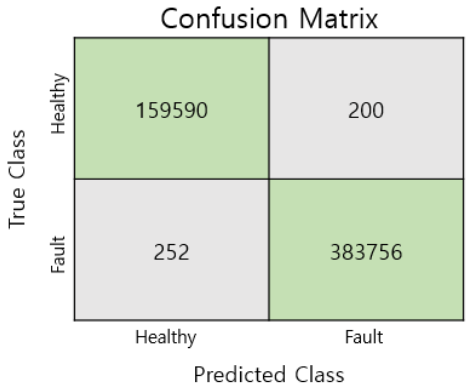

Fig. 16. Confusion matrix of SVM classification result for generating fault flag.

V. Conclusion

In this paper, a fault diagnosis algorithm for an magnetorheological damper is proposed. The proposed fault diagnosis algorithm consists of the damper state observer that estimates the damper states and a support vector machine classifier. Using Takagi-Sugeno fuzzy modeling and unknown input observer scheme, the proposed observer, which is robust against unknown road elevation and the damper faults, is designed. In addition, using the desired damping force and actual damping force generated for machine learning training, this paper combines a model-based state estimation method with machine learning based fault diagnosis. This paper also validates the performance of the Takagi-Sugeno fuzzy observer and support vector machine based fault flag generation using a quarter-car test rig, commercial sensors, and an magnetorheological damper. From the results, it is confirmed that the features used for support vector machine training are well estimated. In addition, the data preprocessing process makes the training accurate. Furthermore, it is verified that the support vector machine based fault determination has high accuracy for various road inputs by comparing with the fixed threshold method. This paper provides the following contributions. First, the proposed fault diagnosis algorithm considers a practical suspension sensor system. A commercial accelerometer employed in practical fields is used to verify the performance of the fault diagnosis algorithm. In addition, using a quarter-car test rig and commercial accelerometers, the practicality of the proposed fault diagnosis algorithm is confirmed. Next, the Takagi-Sugeno fuzzy quarter car model has an unmeasured premise variable, whereas this paper proposed a stable damper state observer. Finally, this paper verified that the support vector machine based fault determination can replace the heuristically tuned threshold or map. It thus becomes possible to reduce the effort required to design fault diagnosis algorithms. In conclusion, the proposed fault diagnosis algorithm can be used to detect the damper condition in a vehicle suspension using only two accelerometers.

In this paper, the damper fault is defined as the difference between desired damping force and actual damping force. This definition is suitable for fault detection, however, not for fault isolation. For example, the proposed algorithm cannot find the cause of errors such as damper leaks, electromagnetic coil failures. In terms of future work, the proposed algorithm can be utilized for the damper prognosis. In the field of prognosis, the remaining useful life is determined by the characteristics of the physical system. The difference between the actual damping force and the desired damping force is a reasonable feature of damper performance degradation.

Acknowledgment

This work was supported by the Technology Innovation Program (or Industrial Strategic Technology Development Program-Development of the Core System Technology for Hyper-safe Driving Platform) (20015831, Development of Hyper-safe Driving Platform based on Cooperative Domain Control) funded By the Ministry of Trade, Industry & Energy(MOTIE, Korea); the BK21+ program through the NRF funded by the Ministry of Education of Korea; the National Research Foundation of Korea(NRF) grant funded by the Korea government(MSIP) (No. 2017R1A2B4004116)

REFERENCES

[1] R. Darus and Y. M. Sam, "Modeling and control active suspension system for a full car model," in *2009 5th International Colloquium on Signal Processing & Its Applications*. IEEE, 2009, pp. 13–18.

[2] S. M. Savaresi and C. Spelta, "A single-sensor control strategy for semi-active suspensions," *IEEE Transactions on control systems Technology*, vol. 17, no. 1, pp. 143–152, 2008.

[3] W. Kim, J. Lee, S. Yoon, and D. Kim, "Development of mando's new continuously controlled semi-active suspension system," SAE Technical Paper, Tech. Rep., 2005.

[4] A. M. Tusset, M. Rafikov, and J. M. Balthazar, "An intelligent controller design for magnetorheological damper based on a quarter-car model," *Journal of Vibration and Control*, vol. 15, no. 12, pp. 1907–1920, 2009.

[5] J. de Jesus Lozoya-Santos, R. Morales-Menendez, J. C. Tudón-Martínez, O. Sename, L. Dugard, and R. Ramirez-Mendoza, "Control strategies for an automotive suspension with a mr damper," *IFAC Proceedings Volumes*, vol. 44, no. 1, pp. 1820–1825, 2011.

[6] H. Du, J. Lam, K. Cheung, W. Li, and N. Zhang, "Direct voltage control of magnetorheological damper for vehicle suspensions," *Smart Materials and Structures*, vol. 22, no. 10, p. 105016, 2013.

[7] M. Khalid, R. Yusof, M. Joshani, H. Selamat, and M. Joshani, "Nonlinear identification of a magneto-rheological damper based on dynamic neural networks," *Computer-Aided Civil and Infrastructure Engineering*, vol. 29, no. 3, pp. 221–233, 2014.

[8] R. Jeyasenthil, S.-B. Choi *et al.*, "Response time effect of magnetorheological dampers in a semi-active vehicle suspension system: performance assessment with quantitative feedback theory," *Smart Materials and Structures*, vol. 28, no. 5, p. 054001, 2019.

[9] Z. Gao, C. Cecati, and S. X. Ding, "A survey of fault diagnosis and fault-tolerant techniques—part i: Fault diagnosis with model-based and signal-based approaches," *IEEE Transactions on Industrial Electronics*, vol. 62, no. 6, pp. 3757–3767, 2015.

[10] J. de Jesus Lozoya-Santos, J. C. Tudón-Martínez, R. Morales-Menendez, R. Ramirez-Mendoza, and L. E. Garza-Castanón, "A fault detection method for an automotive magneto-rheological damper," *IFAC Proceedings Volumes*, vol. 45, no. 20, pp. 1209–1214, 2012.

[11] X. Dong, M. Yu, and Z. Guan, "Adaptive sliding mode fault-tolerant control for semi-active suspension using magnetorheological dampers," *Journal of intelligent material systems and structures*, vol. 22, no. 15, pp. 1653–1660, 2011.

[12] S. Varrier, R. Morales-Menendez, J. D.-J. Lozoya-Santos, D. Hernandez, J. M. Molina, and D. Koenig, "Fault detection in automotive semi-active suspension: Experimental results," SAE Technical Paper, Tech. Rep., 2013.

[13] D. Hernandez-Alcantara, R. Morales-Menendez, L. Amezquita-Brooks, O. Sename, and L. Dugard, "Fault estimation methods for semi-active suspension systems," in *2015 IEEE International Autumn Meeting on Power, Electronics and Computing (ROPEC)*. IEEE, 2015, pp. 1–5.

[14] J. C. Tudon-Martinez and R. Morales-Menendez, "Adaptive vibration control system for mr damper faults," *Shock and Vibration*, vol. 2015, 2015.

[15] H. Kim and H. Lee, "Height and leveling control of automotive air suspension system using sliding mode approach," *IEEE Transactions on Vehicular Technology*, vol. 60, no. 5, pp. 2027–2041, 2011.

[16] B. Spencer Jr, S. Dyke, M. Sain, and J. Carlson, "Phenomenological model for magnetorheological dampers," *Journal of engineering mechanics*, vol. 123, no. 3, pp. 230–238, 1997.

[17] C.-M. Chang, S. Strano, and M. Terzo, "Modelling of hysteresis in vibration control systems by means of the bouc-wen model," *Shock and Vibration*, vol. 2016, 2016.

[18] A. Turnip, K.-S. Hong, and S. Park, "Control of a semi-active mr-damper suspension system: A new polynomial model," *IFAC Proceedings Volumes*, vol. 41, no. 2, pp. 4683–4688, 2008.

[19] G. Hu, Q. Liu, R. Ding, and G. Li, "Vibration control of semi-active suspension system with magnetorheological damper based on hyperbolic tangent model," *Advances in Mechanical Engineering*, vol. 9, no. 5, p. 1687814017694581, 2017.

[20] M. Jesussek and K. Ellermann, "Fault detection and isolation for a nonlinear railway vehicle suspension with a hybrid extended kalman filter," *Vehicle System Dynamics*, vol. 51, no. 10, pp. 1489–1501, 2013.

[21] M. Li, Y. Zhang, and Y. Geng, "Fault-tolerant sliding mode control for uncertain active suspension systems against simultaneous actuator and sensor faults via a novel sliding mode observer," *Optimal Control Applications and Methods*, vol. 39, no. 5, pp. 1728–1749, 2018.

[22] K. Mehran, "Takagi-sugeno fuzzy modeling for process control," *Industrial Automation, Robotics and Artificial Intelligence (EEE8005)*, vol. 262, 2008.

[23] X. Tang, H. Du, S. Sun, D. Ning, Z. Xing, and W. Li, "Takagi–sugeno fuzzy control for semi-active vehicle suspension with a magnetorheological damper and experimental validation," *IEEE/ASME transactions on mechatronics*, vol. 22, no. 1, pp. 291–300, 2016.

[24] L. C. Félix-Herrán, D. Mehdi, J. d. J. Rodriguez-Ortiz, R. Soto, and R. Ramírez-Mendoza, "Takagi-sugeno fuzzy model of a semi-active suspension with a magnetorheological damper," in *2009 European Control Conference (ECC)*. IEEE, 2009, pp. 4422–4427.

[25] X.-H. Chang and G.-H. Yang, "A descriptor representation approach to observer-based h_∞ control synthesis for discrete-time fuzzy systems," *Fuzzy Sets and Systems*, vol. 185, no. 1, pp. 38–51, 2011.

[26] L. K. Wang, J. L. Peng, X. D. Liu, and H. G. Zhang, "An approach to observer design of continuous-time takagi–sugeno fuzzy model with bounded disturbances," *Information Sciences*, vol. 324, pp. 108–125, 2015.

[27] W. Chen and M. Saif, "Design of a ts based fuzzy nonlinear unknown input observer with fault diagnosis applications," in *2007 American Control Conference*. IEEE, 2007, pp. 2545–2550.

[28] M. Lungu, "Design of reduced-order multiple observers for takagi-sugeno systems with unknown inputs," *Measurement*, vol. 134, pp. 710–720, 2019.

[29] D. Ichalal, B. Marx, J. Ragot, and D. Maquin, "Fault detection, isolation and estimation for takagi–sugeno nonlinear systems," *Journal of the Franklin Institute*, vol. 351, no. 7, pp. 3651–3676, 2014.

[30] P. Bergsten, R. Palm, and D. Driankov, "Observers for takagi-sugeno fuzzy systems," *IEEE Transactions on Systems, Man, and Cybernetics, Part B (Cybernetics)*, vol. 32, no. 1, pp. 114–121, 2002.

[31] D. Rotondo, M. Witczak, V. Puig, F. Nejjari, and M. Pazera, "Robust unknown input observer for state and fault estimation in discrete-time takagi–sugeno systems," *International Journal of Systems Science*, vol. 47, no. 14, pp. 3409–3424, 2016.

[32] M. Chadli and H. R. Karimi, "Robust observer design for unknown inputs takagi–sugeno models," *IEEE Transactions on Fuzzy Systems*, vol. 21, no. 1, pp. 158–164, 2012.

[33] D. Ichalal, B. Marx, J. Ragot, and D. Maquin, "Design of observers for takagi-sugeno systems with immeasurable premise variables: an $l2$ approach," *IFAC Proceedings Volumes*, vol. 41, no. 2, pp. 2768–2773, 2008.

[34] T. M. Guerra, R. Márquez, A. Kruszewski, and M. Bernal, "h_∞ lmi-based observer design for nonlinear systems via takagi–sugeno models with unmeasured premise variables," *IEEE Transactions on Fuzzy Systems*, vol. 26, no. 3, pp. 1498–1509, 2017.

[35] V.-P. Vu, W.-J. Wang, and P.-J. Lee, "Observer design for uncertain ts fuzzy system with multiple output matrices and unmeasurable premise variables," in *2016 IEEE International Conference on Fuzzy Systems (FUZZ-IEEE)*. IEEE, 2016, pp. 1910–1917.

[36] A. N. Kiss, B. Marx, G. Mourot, G. Schutz, and J. Ragot, "Observers design for uncertain takagi–sugeno systems with unmeasurable premise variables and unknown inputs. application to a wastewater treatment plant," *Journal of Process Control*, vol. 21, no. 7, pp. 1105–1114, 2011.

[37] D. Ichalal, B. Marx, D. Maquin, and J. Ragot, "On observer design for nonlinear takagi-sugeno systems with unmeasurable premise variable," in *2011 International Symposium on Advanced Control of Industrial Processes (ADCONIP)*. IEEE, 2011, pp. 353–358.

[38] H. Moodi and M. Farrokhi, "On observer-based controller design for sugeno systems with unmeasurable premise variables," *ISA transactions*, vol. 53, no. 2, pp. 305–316, 2014.

[39] S. Gómez-Peñate, G. Valencia-Palomo, F.-R. López-Estrada, C.-M. Astorga-Zaragoza, R. A. Osornio-Rios, and I. Santos-Ruiz, "Sensor fault diagnosis based on a sliding mode and unknown input observer for takagi-sugeno systems with uncertain premise variables," *Asian Journal of Control*, vol. 21, no. 1, pp. 339–353, 2019.

[40] G.-R. Duan and H.-H. Yu, *LMIs in control systems: analysis, design and applications*. CRC press, 2013.

[41] F. Zhang, *The Schur complement and its applications*. Springer Science & Business Media, 2006, vol. 4.

[42] T. Evgeniou and M. Pontil, "Support vector machines: Theory and applications," in *Advanced Course on Artificial Intelligence*. Springer, 1999, pp. 249–257.

[43] A. Widodo and B.-S. Yang, "Support vector machine in machine condition monitoring and fault diagnosis," *Mechanical systems and signal processing*, vol. 21, no. 6, pp. 2560–2574, 2007.

[44] S. Kotsiantis, D. Kanellopoulos, and P. Pintelas, "Data preprocessing for supervised leaning," *International Journal of Computer Science*, vol. 1, no. 2, pp. 111–117, 2006.

Kicheol Jeong received his B.S. degree in Mechanical Engineering from Hanyang University, Seoul, South Korea, and M.S. in Mechanical Engineering from the Korea Advanced Institute of Science and Technology (KAIST), Korea and the Ph.D degree in Mechanical Engineering from the KAIST, in 2021. Since 2021, he has been with the Senior researcher of Korea Automotive Technology Institute. His research interests include vehicle dynamics and control, fault diagnosis and control theory.

Seibum B. Choi received B.S. degree in mechanical engineering from Seoul National University, Korea, M.S. degree in mechanical engineering from Korea Advanced Institute of Science and Technology (KAIST), Korea, and the Ph.D. degree in controls from the University of California, Berkeley in 1993. Since 2006, he has been with the faculty of the Mechanical Engineering department at KAIST. His research interests include fuel saving technology, vehicle dynamics and control, and application of self-energizing mechanism.